Acta Scientiarum

http://www.uem.br/acta
ISSN printed: 1806-2563
ISSN on-line: 1807-8664
Doi: 10.4025/actascitechnol.v35i4.15712

Temperature distributions in pavement and bridge slabs heated by using vertical ground-source heat pump systems

Asim Balbay[1*] and Mehmet Esen[2]

*[1]Department of Mechanical Engineering, Faculty of Engineering and Architecture, Siirt University, 56100, Siirt, Turkey. [2]Department of Automotive Engineering, Faculty of Technology, Firat University, Elazıg, Turkey. *Author for correspondence. E-mail: asimbalbay@gmail.com; abalbay@siirt.edu.tr*

ABSTRACT. Temperature distribution which occurs in pavement and bridge slabs heated for de-icing and snow melting during cold periods is determined by using vertical ground-source heat pump (GSHP) systems with U-tube ground heat exchanger (GHE). The bridge and pavement models (slabs) for de-icing and snow melting were constructed. A three-dimensional finite element model (FEM) was developed to simulate temperature distribution of bridge slab (BS) and pavement slab (PS). The temperature distribution simulations of PS and BS were conducted numerically by computational fluid dynamics (CFD) program named 'Fluent'. Congruence between the simulations and experimental data was determined.

Keywords: de-icing and snow melting, ground-source heat pump, ground heat exchanger, borehole, finite element method.

Distribuições de temperatura no pavimento e ponte lajes aquecidas usando um sistema vertical de bomba de calor derivado da terra

RESUMO. O objetivo deste estudo foi determinar e apresentar a distribuição de temperatura que ocorre em lajes de pavimento e ponte quando aquecidos para o degelo e o derretimento da neve em épocas frias, utilizando um sistema vertical de bomba de calor derivado da terra, com tubo em U de trocador de calor derivado da terra. Foram construídos os modelos de ponte e calçada (lajes) para degelo e o derretimento da neve. Um modelo tridimensional de elementos finitos foi desenvolvido para simular a distribuição da temperatura da laje da ponte (BS) e a laje do pavimento (PS). As simulações de temperatura de distribuição de PS e BS foram calculadas numericamente pelo programa computacional de dinâmica de fluidos, chamado 'Fluent'. Determinou-se a congruência entre as simulações e os dados experimentais.

Palavras-chave: degelo e derretimento da neve, bomba de calor derivado da terra, trocador de calor da terra, perfuração, método dos elementos finitos.

Introduction

Many efforts to prevent pavement and bridge decks from icing have been made in the past years and alternatives are still being researched. Among numerous approaches, spreading salt and/or sand or other gritty material on the pavement and bridge surfaces is the most conventional and popular way on account of the low cost. However, ice will not be melted by the most popularly used salt (sodium chloride) if the temperature falls below 25°F (-3.9°C). In addition, the use of salt results in corrosion of the paint, structural steel, and reinforcing steel embedded in concrete of bridge deck, and eventually will necessitate the rehabilitation or replacement of the bridge deck. To avoid these problems, using a heating system to melt snow and prevent pavement and bridge icing has been proposed in the past decades as an alternative to spreading salt (BALBAY; ESEN, 2010; GAO et al., 2010; LUND, 2000; WANG el al., 2008). The available technologies for bridge and pavement heating generally fall into three groups: hydronic, heat pipe, and electrical. Among the three available heating technologies, hydronic heating is the most promising candidate to be practically applied for the applications of bridge and pavement snow melting.

This is due to certain inherent advantages compared to other systems. It is possible that the heat used in the hydronic heating system is extracted from ground or ground water using the ground source heat pump (GSHP). Such systems generally have higher energy efficiency than boilers or electrical heaters. Snow/ice melting by geothermal water and ground source heat pump is used in several countries, including Iceland, Japan, and United States for several decades. In the literature, there are many studies about deicing by using GSHP system (WANG et al., 2010; ZWARYCZ, 2002). However, there are very limited studies using numerical analysis (CHAPMAN, 1999; CHEN et al., 2011; CHIASSON et al., 2000; KILKIS, 1994; LEAL; MILLER, 1972; LIU et al., 2007; REES et al., 2002; TUMIDAJSKI et al., 2003).

In this study, experimental and numerical studies were carried out for determining the temperature distribution of bridge slab (BS) and pavement slab (PS) constructed for analyzing snow melting and deicing on their surfaces. An FEM has been developed for numerical investigation. The effect of borehole depths on the temperature distributions was investigated numerically and experimentally.

Material and methods

Experimental set-up

An experimental facility has been built to investigate the feasibility of using a ground source heat pump to hydronically heat small scale models of a bridge deck and a pavement. A schematic view of the experimental set-up is shown in Figure 1. It principally consists of a vertical GSHP system, two prototype slabs (Bridge-Slab (BS) and Pavement-Slab (PS)), a circulation pump, and pipe circuits. The vertical GSHP system constructed for this study has a three single U-tube ground heat exchanger (GHE) made of polyethylene pipe with 40 mm outside diameter. The main characteristic of high density polyethylene pipe is shown in Table 1. These pipes are preferred because they are light weight, easy mountable, lower material cost and are not subjected to corrosion like metallic pipes. The vertical drilling of borehole for the GSHP unit was performed for three different depths (30, 60, and 90 m) and about 150 mm diameter in Elazig (38.41° N, 39.14° E), Turkey. The horizontal distances between the boreholes are 3.4 m (B3–B2) and 2 m (B1–B2) m, respectively (Figure 2). B1 defines the working conditions of the borehole having a depth of 30 m. Similarly B2 defines 60 m and B3 defines 90 m borehole depths. U-tubes were embedded into these holes and spaces between tubes were filled with grout. The thermal response test (TRT) was carried out in B2 and B3. The test is a suitable method to determine the effective thermal conductivity of the underground and borehole thermal resistance. The bridge and pavement models (slabs) for deicing and snow melting have dimension of 1.2 x 1.7 x 0.2 m. The slabs were made of Portland cement concrete and sand. The serpentine pipe configuration is used in these slabs as shown in Figure 3. The embedded hydronic tubing in bridge slab (BS) and pavement slab (PS) is 16 mm outside diameter polyethylene pipe on 0.2 m centers at a depth of 0.07 m. The total length of embedded heating pipes in each slab is 8.3 m. The fluid inlet and outlet pipes are at a distance of 15 cm from the ends of the slab. The pipes have been connected to each other by 'U' shaped rubber tubing. This forms a continuous loop heat exchanger within the slab. An aqueous solution of propylene glycol at 25% concentration by weight is used as the heat carrier fluid circulated in the embedded pipe network of both slabs. These pipes are connected to a ground source heat pump.

The heated solution of the anti-freeze circulated through the pipes hydronically heats the slabs. In the heat pump system, evaporator provides the interaction between anti-freeze solution and Freon-22 (gas) providing heat pump circulation. Freon-22 in evaporator gets heat of anti-freeze solution by the help of heat exchanger and transfers it to condenser by the help of compressor. Freon-22 circulating in condenser transfers heat to anti-freeze solution circulating through BS and PS models. Therefore, snowing and icing in bridge and pavement slabs are provided to decrease as temperature of anti-freeze solution circulating in bridge and pavement slabs increases.

Table 1. The main characteristic of high-density polyethylene U-tube.

Pipe material	SDR-11
Outer diameter	40 mm
Inner diameter	35.2 mm
Density	0.96 g cm^{-3}
Melting temperature	130°C
Working temperature	90°C
Peak temperature (instant)	125°C
Thermal conductivity (λ)	0.4 W $(m\ K)^{-1}$
Thermal resistance (R_b)	0.0815 (m K) W^{-1}
Linear expansion coefficient	0.17 mm $(m\ K)^{-1}$
Wall thickness	2.4 mm

Modeling approach

An important emphasis of the researches on maintaining a surface free of ice or snow for bridge decks and pavements during the whole winter period is the optimal design and control of these systems. Reliable mathematical models of all the system components are required in order to accomplish this task. Testing and validation of the component models are essential to ensure their accuracy and the validity of the system simulation. This study is concerned with validation of the bridge deck and pavement models.

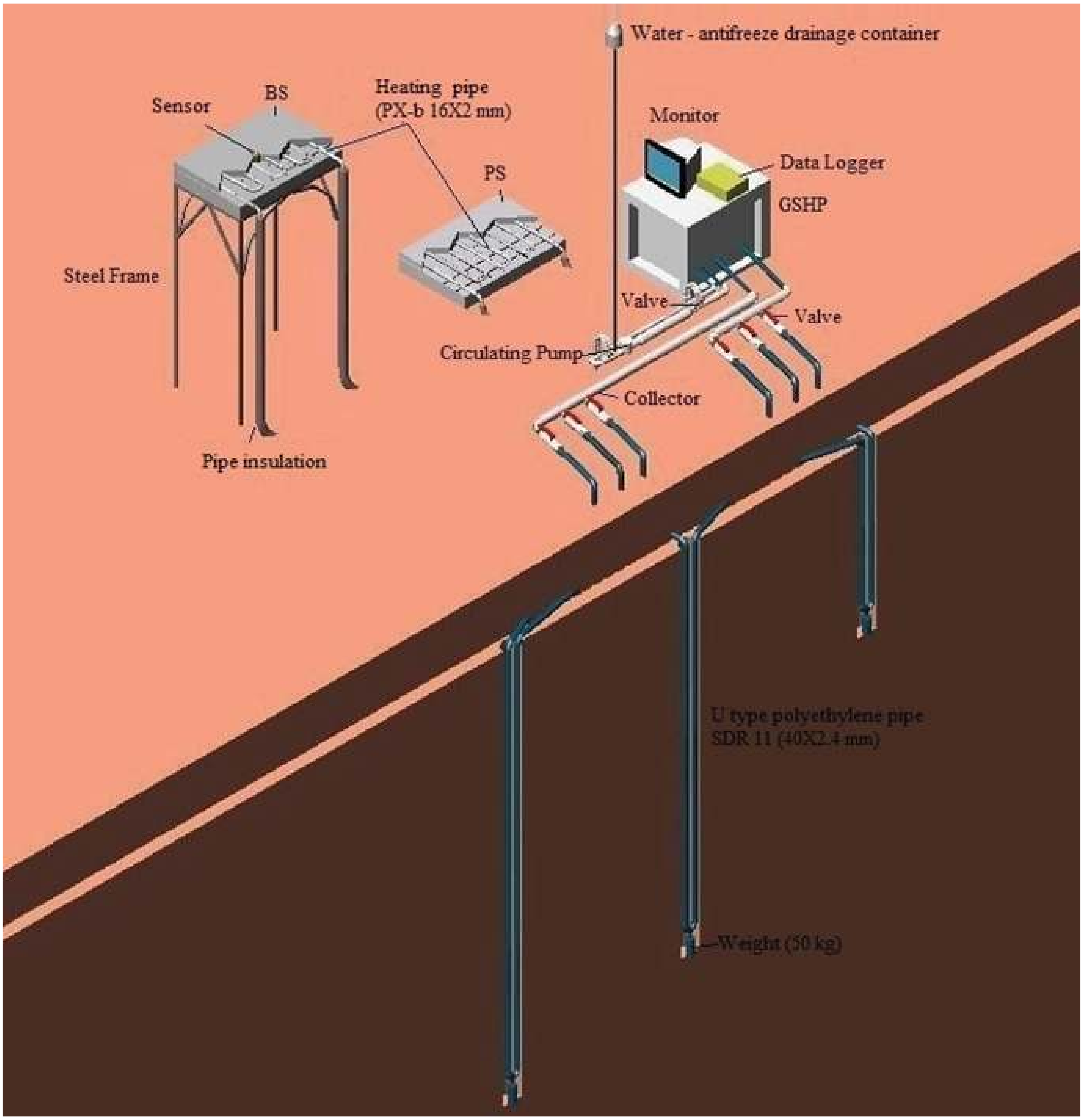

Figure 1. 3D view of experimental set-up.

CFD simulations were performed with FLUENT version 6.2. Meshing was performed within GAMBIT 2.2. Dense mesh was incorporated in the near vicinity of the pipe locations. The 3D mesh consisted of mixed elements with approximately 1 million cells for each slab.

The temperature distribution development was obtained for each slab heated by GSHP system. The temperature distribution simulations of PS and BS were conducted using FLUENT computational fluid dynamics (CFD) package program. The comparisons demonstrate a plausible accord between the numerical and the measured data. The results show that the FEM can be used to predict the temperature distribution development of the GHEs and slabs.

The starting point of any numerical method is the mathematical model, i.e. the set of partial differential equations and boundary conditions. The sets of equations are chosen for target application (inviscid, incompressible, turbulent, two or three dimensional). The continuity equation and the Navier-Stokes equations are needed to obtain the pressure and velocity around the flow field. Note that the fluid-side heat transfer coefficient is computed based on the local flow-field conditions (e.g., turbulence level, temperature, and velocity profiles).

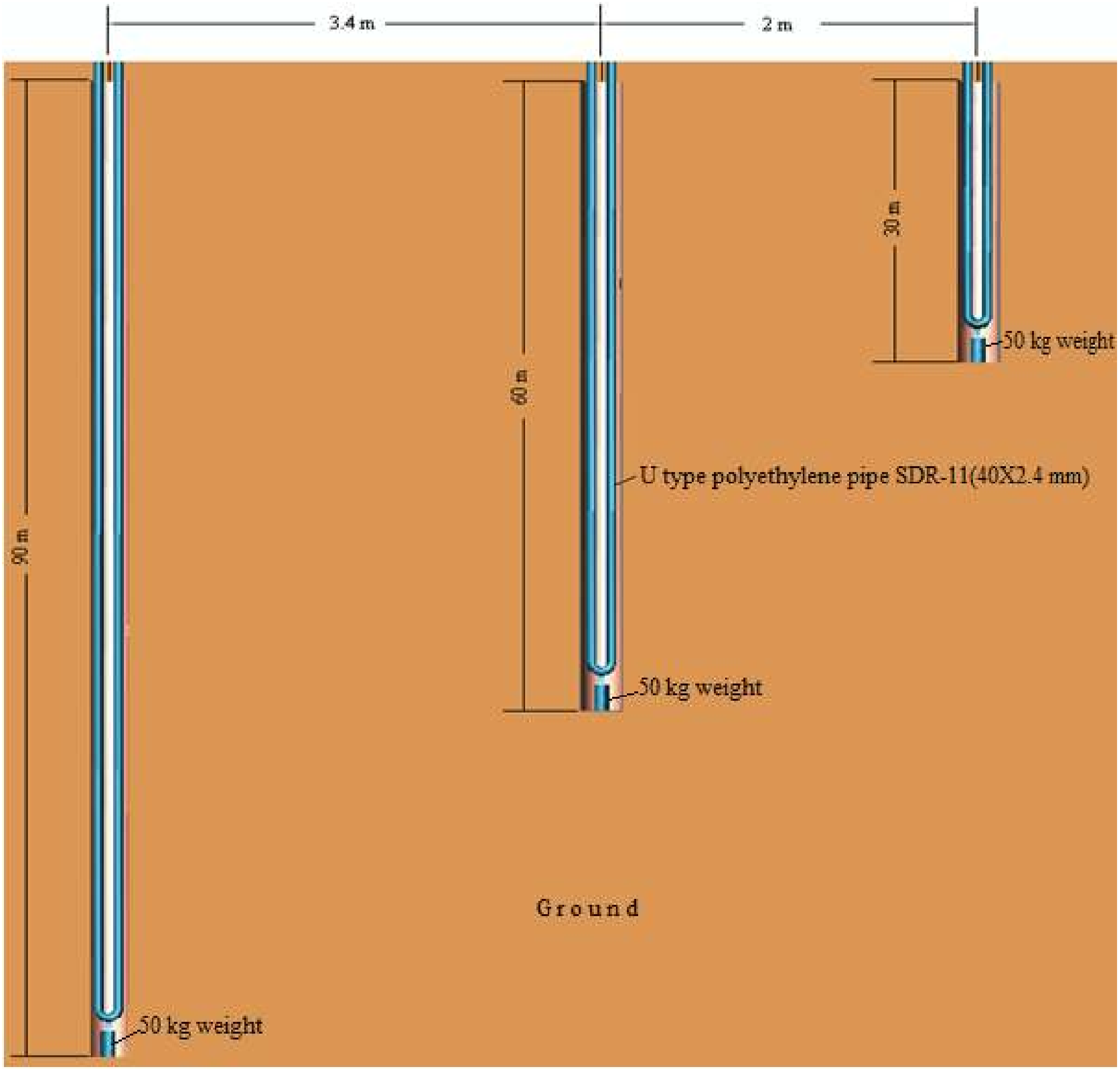

Figure 2. The schematic view of depths of boreholes and distances between boreholes.

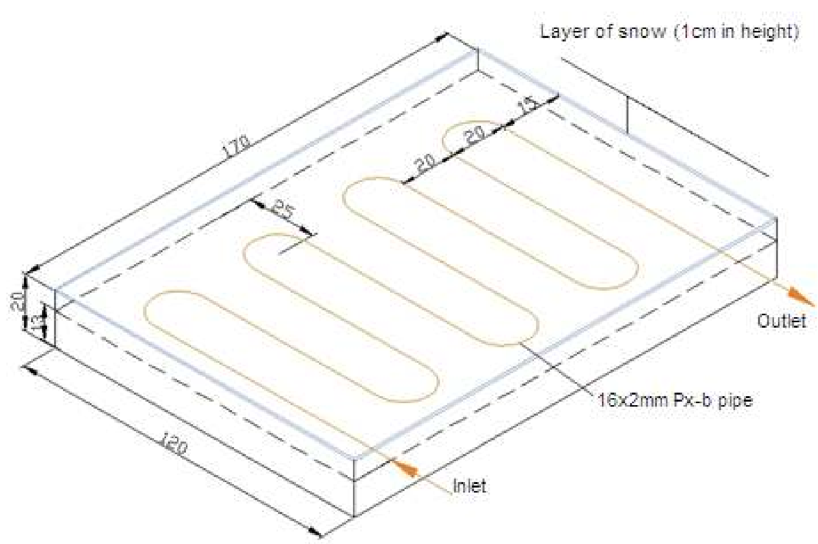

Figure 3. Dimensions of the bridge and pavement models.

PS and BS model

After creating the geometric model and defining the necessary parameters including the material thermal properties, the element size and type as well as boundary conditions, the Gambit program can automatically generate an FEM which consist of nodes and elements, as shown in Figure 4. The region nearest to the pipes, where the temperature gradient is the steepest, is more finely meshed to enable the temperatures to be accurately predicted, as shown in Figure 4. Gambit software, which is a preprocessor, can be used in Finite Element Analysis (FEA) and CFD analysis. Then created models in Gambit software are exported to the Fluent software in which the viscous model, boundary conditions and material properties are defined.

A standard k-ε model is used to predict turbulent flow in pipe. After the FEM is built with the mesh discretisation, the temperature distribution development problem can be solved numerically.

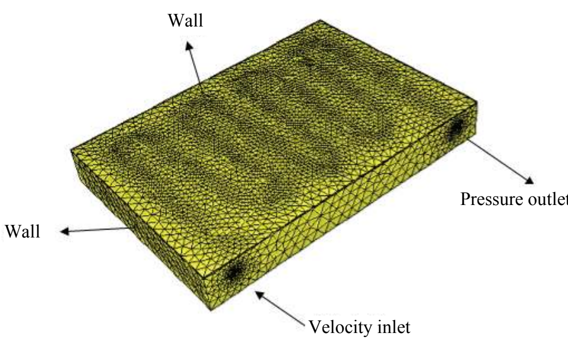

Figure 4. The meshed model of the PS ve BS.

The models are created and meshed depend on the laws of conservation of mass and energy and use basic thermodynamic and heat transfer correlations. Velocity inlet and pressure outlet are used to define the velocity properties of the flow at inlet and outlet boundaries. The velocity inlet of anti-freeze solution to the PS and BS models was chosen 0.07 m s^{-1}, which was obtained from the experiments. The pressure outlet is defined as atmospheric, i.e. zero gage pressure. It is assumed that block edges to be insulated, top side to be opened. Also, it is assumed that there is a snow/ice formation of 1 cm thickness on top surfaces of slabs. Thermal properties of materials used in models are given in Table 2.

The convection heat transfer coefficient (h_c) is taken as the upper limit between the free and forced convection coefficients. The following equations are used in order to calculate convection heat transfer coefficient for top and bottom of slabs (INCROPERA; DEWITT, 1996).

Table 2. Thermophysical properties of materials used in models.

Materials	Density ($kg\ m^{-3}$)	Specific heat ($J\ kg\ K^{-1}$)	Thermal conductivity ($W\ m\ K^{-1}$)
anti-freeze solution	1111	3700	0.25
Snow	200-600	1500	0.03-0.6
Ice	917 (0°C)	1960 (0°C)	2.0-2.1
Concrete	2300	880	1.4
PEX pipe	950	1800	0.41
Air	1.225	1006.43	0.0242

$$Nu=0.664Re^{1/2}\ Pr^{1/3} \text{ (Laminar flow regime)} \quad (1)$$

$$Nu=0.037Re^{4/5}\ Pr^{1/3} \text{ (Mixed and turbulent flow regimes)} \quad (2)$$

$$h_c = \frac{Nu.k_{air}}{L} \quad (3)$$

Equation 6 is obtained by substituting equation 2 in equation 3.

$$h_c = 0.037(\frac{k_{air}}{L})Re_L^{0.8}.Pr^{1/3} \quad (4)$$

$$Re_L = \frac{VL}{\nu_{air}}c_2 \quad (5)$$

The temperatures of top and bottom surfaces of slab were considered as -7°C in the beginning of tests. The mean temperature of antifreeze solution at inlet of model slabs is about 36°C, which were obtained from the experimental study. Radiation heat transfer, wind direction, snowing, raining, and humidity of air were neglected.

The thermal conductivity of the grout was obtained λ = 1.70 W mK^{-1} as result of thermal responsibility test, nevertheless the thermal conductivity of the ground in the vicinity of borehole is 2.55 W m K^{-1}. The undisturbed temperature of ground in depth of 30 m is approximately 15-18°C.

Since wind speed value was not able to enter to program directly; convection heat transfer coefficient was calculated depending on the wind speed. Convection heat transfer coefficient was calculated as 28.22 W m^2 K^{-1} with average wind speed value of 1.9 m s^{-1} (6.84 km h^{-1}) in Elazig in 2006 (ELAZIĞ STATE METEOROLOGICAL STATION, 2005-2006).

Results and discussion

Temperature distributions in BS and PS for different borehole depths (30, 60, and 90 m) are shown in Figures 5, 6 and 7, respectively. As can be seen figures, the temperature distributions were uniform in PS and BS. Average temperature differences between inlet and outlet of fluid in PS and BS were calculated 0.93 and 0.67°C for borehole of B1, 0.98 and 0.71°C for B2, 1.04 and 0.75°C for B3, respectively.

An unsteady state study was performed in order to melt snow or ice by GSHP system for borehole depths of 30, 60 and 90 m. In this study, three dimensional drawing and boundary conditions were defined in Gambit and then unsteady state solution of bridge and pavement slab models was investigated by the help of Fluent 6.2. Fluent program was run by 'Iterate' command as 'Initialize' option under 'Solve' menu to be activated. 'Time Step Size(s)' option in Iterate menu was taken as 0.1.

The unsteady state analysis of PS surface temperatures for borehole depth of 30m can be observed from the Figure 8. Temperature distributions within the slabs for heating mode are reasonably smooth.

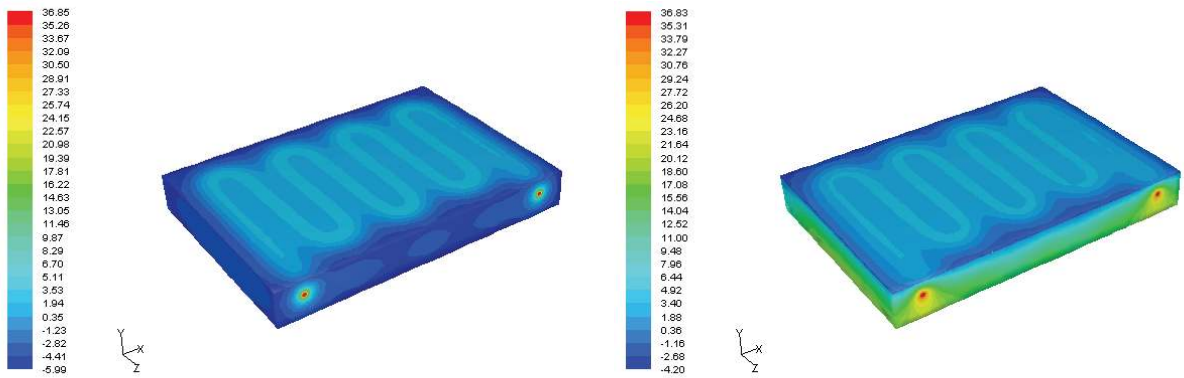

Figure 5. Temperature distribution of PS (left side) and BS (right side) (30 meters).

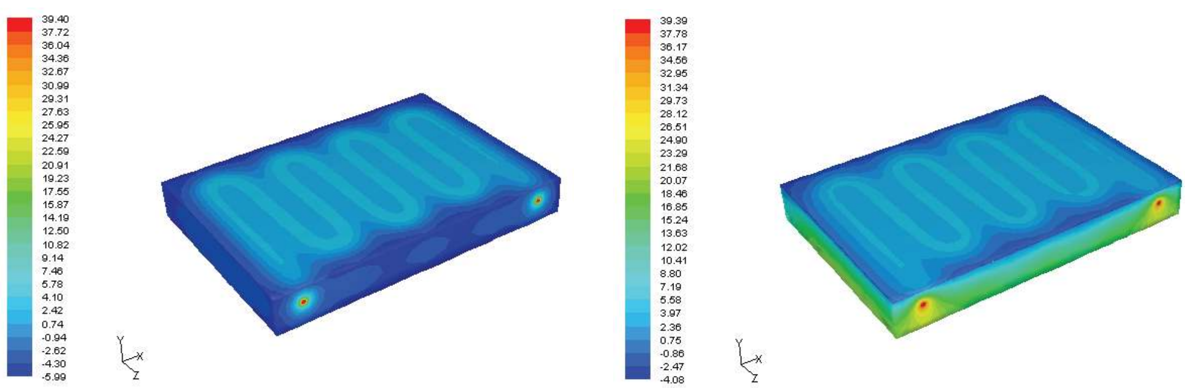

Figure 6. Temperature distribution of PS (left side) and BS (right side) (60 meters).

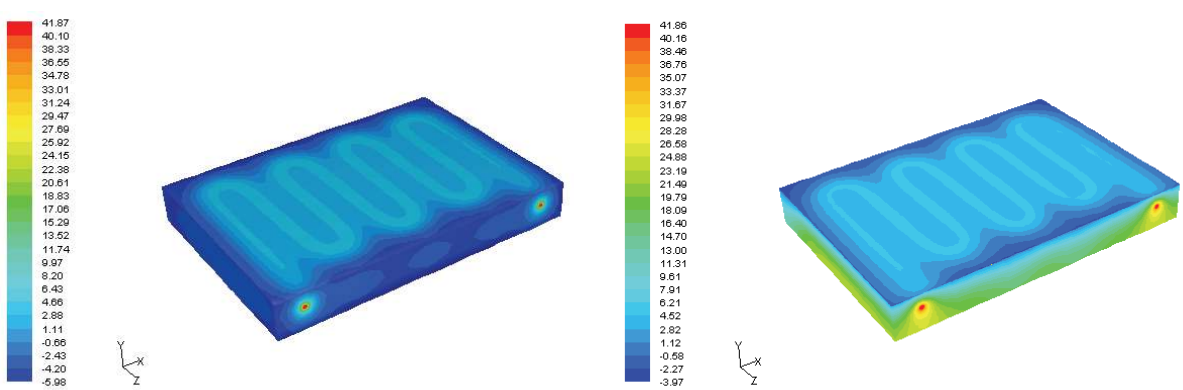

Figure 7. Temperature distribution of PS (left side) and BS (right side) (90 meters).

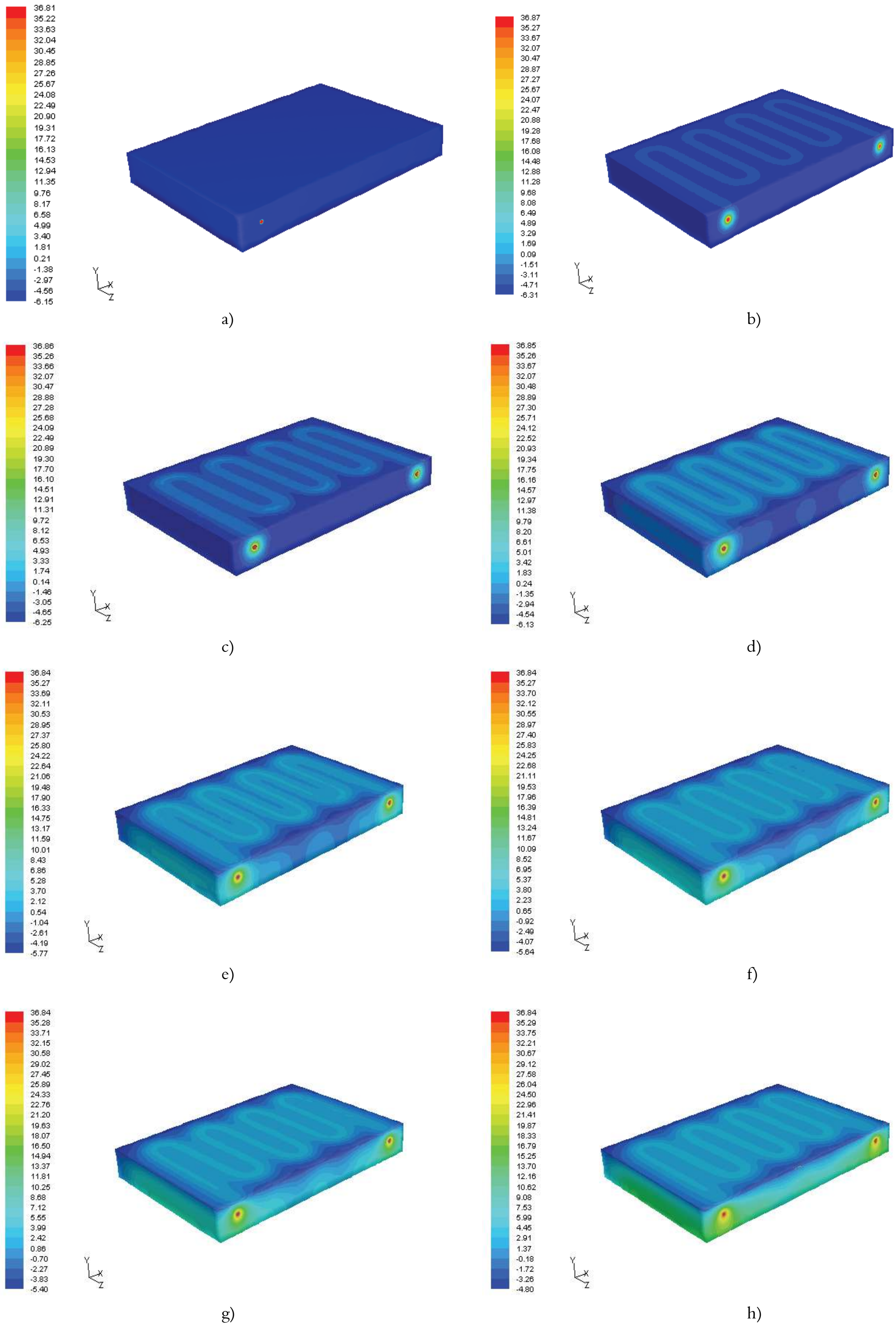

a) 0 s b) 3600 s c) 7200 s d) 10800 s e) 14400 s f) 18000 s g) 21600 s h) 25200 s

Figure 8. UnsteaLdy state temperature distribution of PS.

The average surface temperature difference between the surfaces of BS and PS was calculated as 0.9 and 0.6°C for 3 and 7 hours later from the beginning of the solution. The average inlet and outlet temperature difference of anti-freeze solution were 1.4 and 0.7°C in BS and PS, respectively for 3 hours later from the beginning of the solution, while they are 1.1 and 0.8°C in BS and PS, respectively for 7 hours later. The average surface temperatures of PS and BS as well as the average temperature differences between inlet and outlet of anti-freeze solution are given experimentally and theoretically in Table 3. As the depth of borehole increases, the temperature difference of anti-freeze solution and the average surface temperature of slabs increases in both theoretical and experimental results, as can be seen from Table 3. Approximately 0.4 and 0.5°C improvements, in respectively, in BS and PS surface temperature were obtained in both experimental and computational study for each 30m, in all operated borehole depths (30, 60, and 90 m).

Table 3. Comparison of average surface temperature and average temperature differences in slabs.

	Average surface temperature (°C)			The average temperature difference between inlet and outlet of anti-freeze solution (°C)		
Depths	30 m	60 m	90 m	30 m	60 m	90 m
PS experimental	2.13	2.85	3.3	1.79	1.89	2.98
BS experimental	0.12	0.52	1.15	2.75	2.9	3.08
PS Model	2.51	3.04	3.56	0.67	0.71	0.75
BS Model	0.38	0.78	1.17	0.93	0.98	1.04

Conclusion

In this study, experimental and computational studies were presented in order to analyze the melting of the snow/ice occurred in bridge and pavement surfaces in winter. The data obtained from experimental and theoretical studies are in good agreement. Also, good agreement with literature data was observed.

Thermal properties related to ground structure were found as very important parameters in design of vertical GSHP system. The top surface of BS and PS normally exposed to greater temperature fluctuations than bottom surfaces. Computational program approximately predicted top surface temperatures of models and inlet-outlet temperatures of anti-freeze solution. Convection coefficient of air and thermal conductivity of slabs had significantly effects on surface temperatures. The higher wind speed is, the higher convection heat coefficient at the slab surfaces, resulting lower top surface temperatures.

Nomenclature

GSHP ground source heat pump
GHE ground heat exchanger
PS pavement model
BS bridge model
FEM finite element method
FEA finite element analysis
CFD computer fluid dynamic
B1 30 m borehole
B2 60 m borehole
B3 90 m borehole
k_{air} thermal conductivity of air near block (W m °C^{-1})
L characteristic length of block measured in wind direction (m)
Pr prandtl number of air, Pr = 0.7 taken
Re_L reynolds number dependent on characteristic length L
V design wind speed near block, km h^{-1}
υ_{air} air kinematic viscosity, m^2 s^{-2}
c_2 1000 m km^{-1} x 1 hour 3600 s^{-1} = 0.278.

Acknowledgements

The authors gratefully acknowledge the financial support from the Scientific Research Projects Coordination Unit of Firat University for this study performed under project with grant no.2005/1154.

References

BALBAY, A.; ESEN, M. Experimental investigation of using ground source heat pump system for snow melting on pavements and bridge decks. **Scientific Research and Essays**, v. 5, n. 24, p. 3955-3966, 2010.

CHAPMAN, W. P. A review of snow melting system design. **ASHRAE Transactions**, v. 105, n. 1, p. 1049-1054, 1999.

CHEN, M.; WU, S.; WANG, H.; ZHANG, J. Study of ice and snow melting process on conductive asphalt solar collector. **Solar Energy Materials and Solar Cells**, v. 95, n. 12, p. 3241-3250, 2011.

CHIASSON, A.; SPITLER, J. D.; REES, S. J.; SMITH, M. D. A model for simulating the performance of a pavement heating system as a supplemental heat rejecter with closed-loop ground-source heat pump systems. **ASME Journal of Solar Energy Engineering**, v. 122, n. 4, p. 183-191, 2000.

ELAZIG STATE METEOROLOGICAL STATION. **Records for weather data in Elazıg**. Turkey, 2005-2006.

GAO, Q.; HUANG, Y.; LI, M.; LIU, Y.; YAN, Y. Y. Experimental study of slab solar collection on the hydronic system of road. **Solar Energy**, v. 84, n. 12, p. 2096-2102, 2010.

INCROPERA, F. P.; DEWITT, D. P. **Introduction to heat transfer**. New York: Wiley and Sons Inc., 1996.

KILKIS, I. B. Design of embedded snow-melting systems: part 2, heat transfer in the slab - a simplified model. **ASHRAE Transactions**, v. 100, n. 1, p. 434-441, 1994.

LEAL, M.; MILLER, P. L. An analysis of the transient temperature distribution in pavement heating installations. **ASHRAE Transactions**, v. 78, n. 2, p. 61-66, 1972.

LIU, X.; REES, S. J.; SPITLER, J. D. Modeling snow melting on heated pavement surfaces. Part I: Model development. **Applied Thermal Engineering**, v. 27, n. 27, p. 1115-1124, 2007.

LUND, J. W. Pavement snow melting. **Geo-Heat Center Quarterly Bulletin**, v. 21, n. 2, p. 12-19, 2000.

REES, S. J.; SPITLER, J. D.; XIAO, X. Transient analysis of snow melting system performance. **ASHRAE Transactions**, v. 108, n. 2, p. 406-423, 2002.

TUMIDAJSKI, P. J,; XIE, P.; ARNOTT, M.; BEAUDOIN, J. J. Overlay current in a conductive concrete snow melting system. **Cement and Concrete Research**, v. 33, n. 11, p. 1807-1809, 2003.

WANG, H.; LIU, L.; CHEN, Z. Experimental investigation of hydronic snow melting process on the inclined pavement. **Cold Regions Science and Technology**, v. 63, n. 1-2, p. 44-49, 2010.

WANG, H.; ZHAO, J.; CHEN, Z. Experimental investigation of ice and snow melting process on pavement utilizing geothermal tail water. **Energy Conversion and Management**, v. 49, n. 6, p. 1538-1546, 2008.

ZWARYCZ, K. Snow melting and heating systems based on geothermal heat pumps at Goleniow Airport, Poland. **Geothermal Training Programme Reports**, n. 21, p. 431-464, 2002.

Received on January 7, 2012.
Accepted on August 1, 2012.